**Stanisław Rabiej**

**University of Bielsko-Biała, Institute of Textile Engineering and Polymer Materials**
Willowa 2, 43-309 Bielsko-Biała, Poland

# WAXS Investigations of the Amorphous Phase Structure in Linear Polyethylene and Ethylene-1-Octene Homogeneous Copolymers

**Abstract**
*Analysis of the position and shape of the amorphous halo in WAXS patterns of linear polyethylene and ethylene-1-octene homogeneous copolymers has shown that the amorphous phase contains regions of macromolecule packing which are enhanced and denser than in the remaining volumes. The disappearance of such partially ordered regions during heating is closely connected with the melting of the crystalline phase. For this reason, the transitional layers on the borders between crystallites and the amorphous phase seem to be the most likely places to find such regions. The presence of side branches (1-octene co-monomers) make the denser packing of macromolecules in these regions more difficult. This fact is clearly reflected in the position of the amorphous halo maximum, which indicates that the average intermolecular distance increases with the increase in concentration of 1-octene.*

**Key words:** *amorphous phase, WAXS curves, amorphous halo, polyethylene, 1-octene, homogeneous copolymers, partially ordered phase.*

## Introduction

Several experimental results published in recent years prove that the amorphous phase of solidified polymers cannot be considered as a direct continuation of the liquid phase existing above the melting temperature. During crystallisation, the structure of the amorphous regions transforms considerably. The measurements of the specific volume of amorphous polyethylene [1] have shown that the latter is already less than the extrapolated liquid specific volume at any given temperature below melting point. This indicates that during solidification the average density of amorphous regions becomes higher than that of liquid polymer. Later, results from solid-state $C_{13}$ NMR [2-6], Raman spectroscopy [7-11], electron microscopy, [12], differential scanning calorimetry (DSC) [13], small-angle (SAXS) and wide-angle (WAXS) X-ray diffraction studies [14-18], have provided subsequent evidence for the creation of semi-ordered, intermediate regions, localised inside the amorphous phase. In this paper, some additional data supporting this hypothesis is presented. It comes from the analysis of the shape and position of the amorphous halo in WAXS patterns of linear polyethylene (LPE) and ethylene-1-octene (EO) homogeneous copolymers with the co-monomer concentration ranging from 0.8 to 9.15 mol%. The results obtained show that during heating, and particularly during melting, clear changes in the structure of the amorphous phase of these polymers take place.

## Experimental

Homogeneous copolymers of ethylene and 1-octene investigated in this work were synthesised at DSM Research (the Netherlands). The samples are listed in Table 1. The sample code for EO copolymers indicates the rounded mole % of 1-octene in a sample. The linear polyethylene (LPE) and EO5 samples were synthesised using a vanadium-based catalyst, and the remaining samples were obtained using a metalocene catalyst system.

The X-ray diffraction patterns of the samples were registered during heating at the rate of 10°C/min, from 20°C up to complete melting. Before the measurements, all the samples were melted at 180°C (or at 160°C in the case of EO7 and EO9 samples) to erase their thermal history and cooled at the same rate of 10°C/min to 20°C. The melting temperatures were established from previous DSC measurements. Time-resolved WAXS investigations were performed using the X33 camera of the EMBL (HASYLAB), on the DORIS storage ring of the Deutsches Elektronen Synchrotron (DESY). The wavelength of X-rays was 1.5 Å. The samples with a thickness of 1mm were sealed between thin aluminium foils. The temperature of the samples was controlled

***Table 1.*** *Investigated samples.*

| Sample | LPE | EO1 | EO2 | EO4 | EO5 | EO6 | EO7 | EO9 |
|---|---|---|---|---|---|---|---|---|
| Mol% of 1-octene | 0 | 0.8 | 1.77 | 4.34 | 5.2 | 5.5 | 6.64 | 9.15 |

***Equation 1.***

$$F_i(x) = f_i H_i \exp\left\{-\ln 2\left[\frac{2(x - x_{oi})}{w_i}\right]^2\right\} + \frac{(1 - f_i)H_i}{1 + [2(x - x_{oi})/w_i]^2} \quad (1)$$

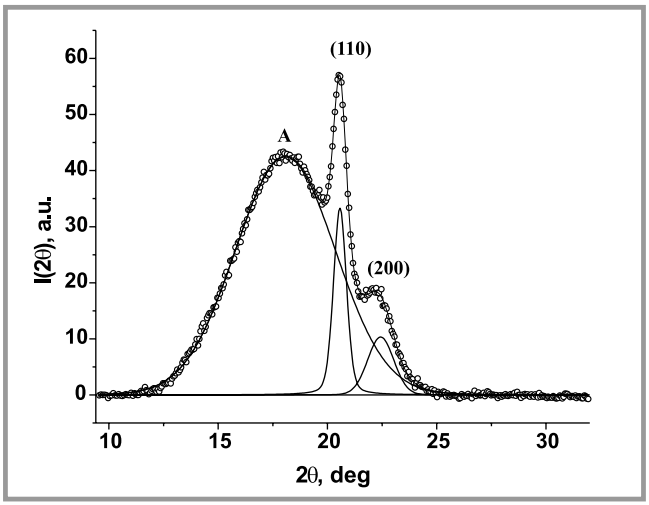


***Figure 1.*** *WAXS pattern of EO4 sample resolved into crystalline peaks (110) and (200) and amorphous halo (A).*

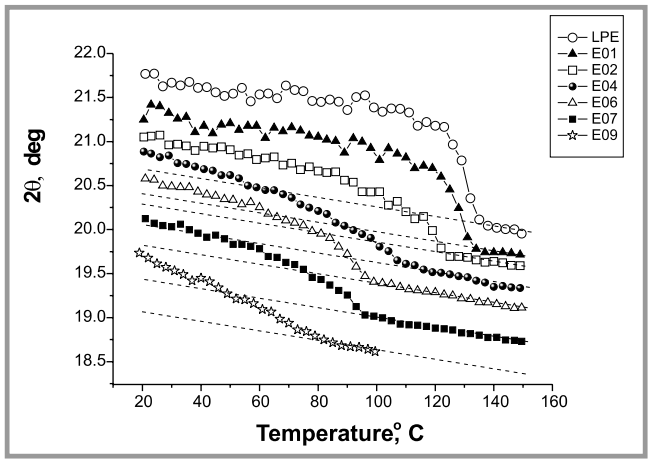


***Figure 2.*** *Amorphous halo position in the WAXS patterns of samples investigated as a function of temperature. The plots are shifted vertically for better visualisation. To reduce the noise, the presented values are averaged over 3 neighbouring data points.*

by a Mettler FP-82HT hot stage. During heating, diffraction patterns were registered every 6s, giving a resolution of 1°C for each pattern. Data processing was preceded by normalisation to the intensity of primary beam and correction for the detector response. Three strong and sharp reflections, 010, 110 and 100 of the β-form of tripalmitin [19], were used for calibration of the 2θ axis. The registration range was $8.35^{o} < 2\theta < 38^{o}$.

**Data elaboration**

After normalisation and Lorentz correction, the WAXS curves were resolved into crystalline peaks and an amorphous halo (Figure 1.) using a new version of the OptiFit computer program [20,22], prepared for the elaboration of real-time experimental data from the synchrotron. In this program, the experimental curve $I_E(x)$ is approximated by a theoretical curve $I_T(x)$, which is a sum of functions describing the crystalline peaks 110 and 200, the amorphous halo and the background. Both the crystalline peaks and the amorphous halo are represented by functions $F_i(x)$, which are linear combinations of Gauss and Lorentz functions: (Equation 1), where $x$ is the scattering angle $2\theta$, $H_i$, $w_i$ and $x_{oi}$ are the peak height, the width at half height, and the peak position respectively. The shape coefficient $f_i$ is equal to 1 for the Gauss profile and 0 for the Lorentz one. The background is described by a third-order polynomial. Fitting the theoretical curve $I_T(x)$ to the experimental one $I_E(x)$ is performed by using a multi-criterial optimisation procedure (the simultaneous minimisation of the sum of squared deviations between the experimental and theoretical curves and the minimisation of the sum of squared deviations between the experimental curve and the component function representing the amorphous halo) and a hybrid algorithm. which combines the genetic algorithm with a classical optimisation method.

By using the program, all the parameters of the component functions were determined, including the position, width and shape factor of the amorphous halo.

## Results and discussion

In Figure 2, the position of the amorphous halo versus temperature for all the samples investigated is shown. It is important to note that above the melting temperature of a given copolymer the plots are nearly linear, and the slope of all lines is very close to one another. Below melting temperatures, one observes a clear deflection from linearity. It should be added that all these plots are shifted vertically versus one another for better visualisation.

In reality, the differences in the intercepts of these lines are very small - the difference between the smallest and the highest is not greater than a quarter of a degree. Taking this into account, and considering the possible experimental, calibrational errors as well as the errors in the resolution procedure, we can assume that for LPE and all copolymers in a liquid state, the dependence of the amorphous halo position on the temperature can be approximated by a single line. To establish this dependence more precisely, one of the copolymers (EO5) was investigated over a broader temperature range, from 100-200°C. The result is shown in Figure 3.

Using the least squares method, the straight line best fitted to the data from Figure 3 was found, and all curves from the previous figure were shifted to this line. The result obtained is shown in Figure 4.

As the amorphous halo is related to the intermolecular interferences [18,23,24], its position must be dependent on the degree of packing of molecules in the amorphous phase. According to Alexander [25], the dependence of the amorphous halo position on the most frequently occurring intermolecular distance can be approximated by the following equation:

$$r_a \approx 1.22 \frac{\lambda}{2 \sin \theta_a} \qquad (2)$$

This is a reciprocal dependence, typical of all diffraction phenomena: the smaller the angle, the higher the intermolecular distance, and as a consequence the smaller the density.

So, as results from the plots in Figure 4, the density of amorphous phase decreases during heating (which could be expected), but we can also see that during melting, the type of this dependency clearly changes. It should be emphasised that the temperature at which a given plot becomes linear agrees exactly with the temperature at which the crystallinity of the sample drops to zero.

It can be shown that when the samples are in a liquid state, a precise relation between their density and the amorphous

halo's position can be established. To find this relation, we define a parameter which can be called a packing factor:

$$P = \left[\frac{1}{r}\right]^3 = \left[\frac{2\sin\theta_a}{\lambda}\right]^3 \qquad (3)$$

***P*** is simply a reciprocal of the third power of distance ***r***, which is found directly from Bragg's law by using the position of the amorphous halo $2\theta_a$. Of course, ***r*** is proportional to the distance $r_o$ given by the equation (2): $r = 0.82 \cdot r_0$.

The packing factor can be calculated for the investigated samples at all temperatures, based on the amorphous halo positions from the linear part of the plots. To calculate the density at a given temperature, we can use the experimental relation determined by Swan for liquid linear polyethylene [1]:

$$\frac{1}{d} = 1.136 + 8.85 \cdot 10^{-4} \cdot t \qquad (4)$$

where t is the temperature in degrees centigrade.

As mentioned above, this equation has been established for linear polyethylene, However taking into account that for all liquid samples (including copolymers) the dependence of the amorphous halo position on the temperature can be approximated by a single line, we may assume that the same is valid for their densities, and that equation (4) can also be a good approximation for all of them.

The plot of the packing factor, calculated from eq. (3) versus density, and calculated from eq. (4) is shown in Figure 5. As one can see, they are quite well correlated linearly with one another. The correlation coefficient is very high: R = 0.997. The best fitted line is given by the following equation:

$$P = 0.018 \cdot d - 0.0046 \qquad (6)$$

If the structure of the amorphous phase in a solid and liquid state were the same, this equation would also be valid below melting temperature. With the aim of checking this, all the data from the previous figure (Figure 4) was recalculated, using equations (3) and (6). The values obtained are presented in Figure 6. The plots show the densities of the amorphous phase versus temperature. Solid lines represent densities of liquid and crystalline LPE according to the formulas given by Swan [1].

Using these plots, the densities of amorphous phase at room temperature were

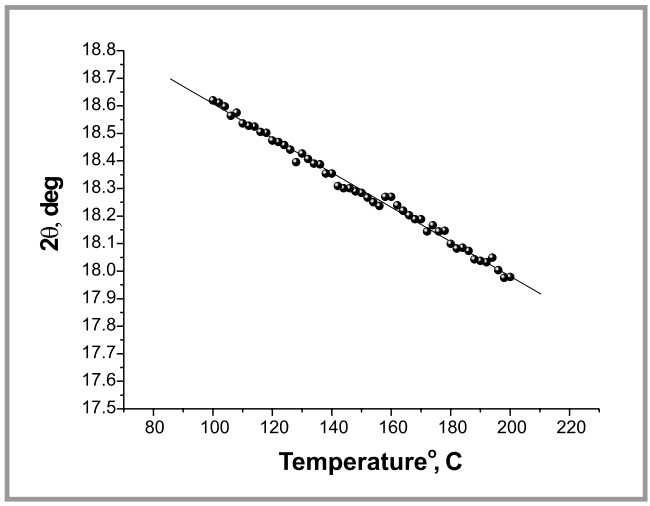


***Figure 3.*** *Position of the amorphous halo of the liquid EO5 sample as a function of temperature.*

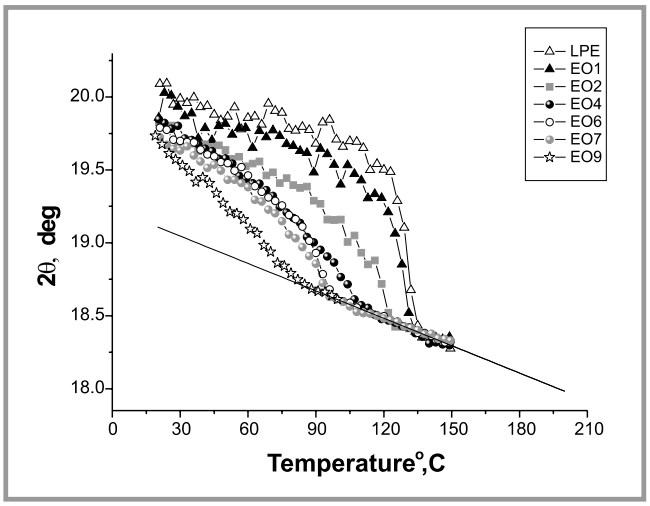


***Figure 4.*** *Amorphous halo position as a function of temperature. The plots from Figure 4 are shifted to the straight line determined in Figure 3.*

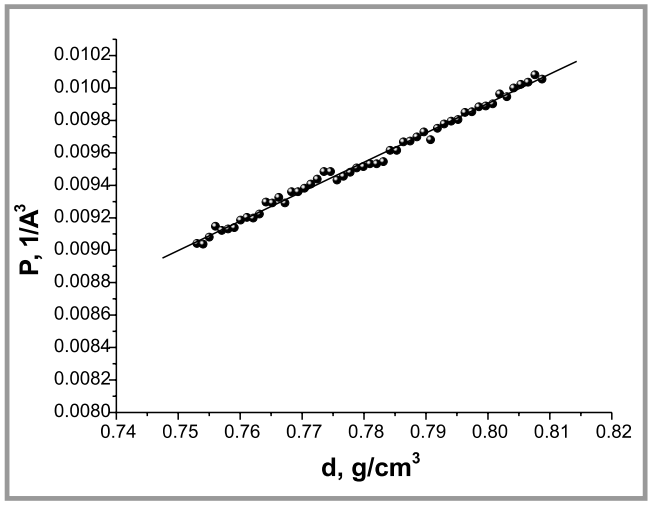


***Figure 5.*** *Packing factor of a liquid copolymer sample plotted versus its density as determined from Swan's equation.*

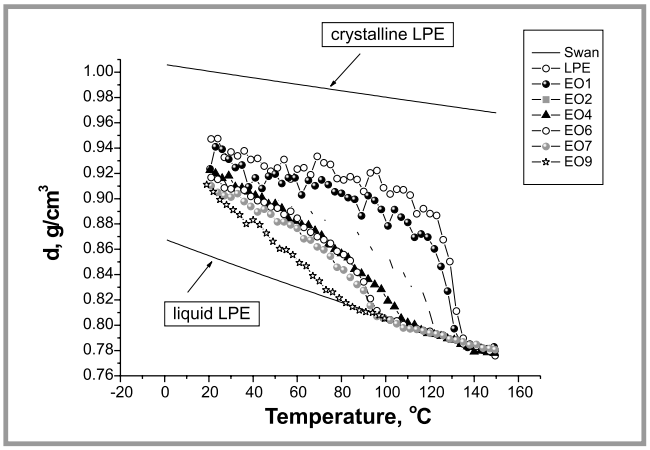


***Figure 6.*** *Density of the amorphous phase of investigated samples as determined from the amorphous halo position (Figure 4) using equations (3) and (6). Solid lines represent the density of crystalline and liquid PE calculated from equations given by Swan [1].*

found and compared with the densities of copolymers at this temperature as given by the producer. The results are given in Table 2.

We can see that obtained values are greater or only slightly smaller than the total densities of copolymers. They can therefore not be the real densities of the amorphous phase. This means that during solidification, some changes in the structure of the amorphous phase take place, and the relation between amorphous halo position and density which was established for a liquid state is not valid for a solid state. Most probably, in this case, the position of amorphous halo is not representative of the whole amorphous phase. The deflection of the plots towards higher angles clearly shows that some denser regions must be present inside the amorphous phase of a solid polymer, and that the total amorphous scattering is composed of two parts. One part is related to a liquid-like amorphous phase, and the other to regions of higher molecular order and density. A composed structure of the amorphous scattering is fully confirmed by the plots shown in Figures 7 and 8. The plots illustrate the changes in the half-height width and shape factor of the amorphous halo during heating. The dotted lines indicate temperatures at which the crystallinity of the samples decreases to zero. We can clearly see that the widths abruptly decrease in the vicinity of the melting temperature of a given sample. Similarly, abrupt, step-like changes occur in the case of the shape factor. Most probably, such changes are caused by the disappearance of the partially ordered regions in the amorphous phase which cease to exist when the melting temperature is approached. Surprisingly, in spite of its composed structure, no traces of asymmetry can be seen in the shape of the amorphous halo, which can be fitted very well by symmetric functions both below and above the melting temperature of a given sample. Typical plots for one of the samples are shown in Figure 9.

***Table 2.*** *A comparison of the real densities of copolymers given by the producer with the densities of amorphous phase found from Figure 6.*

| Sample | EO1 | EO2 | EO4 | EO6 | EO7 | EO9 |
|---|---|---|---|---|---|---|
| Copolymer density [g/cm$^3$] | 0.948 | 0.929 | 0.908 | 0.900 | 0.899 | 0.880 |
| Calculated amorphous phase density [g/cm$^3$] | 0.935 | 0.918 | 0.919 | 0.913 | 0.906 | 0.905 |

## Conclusions

The results obtained evidently prove that below melting temperature, the amorphous phase of the samples investigated is not homogeneous. The abruptly decreasing thickness of the amorphous halo and the sudden changes in its shape during melting, as well as the decreasing position of its maximum, suggest that the amorphous phase contains two contributions. The first of them is related to liquid-like regions. The degree of packing of macromolecules in these regions is the same as in a molten sample. The second contribution is related to the better ordered and denser regions which disappear during melting. In the temperature range at which the samples are completely molten, the dependency of the amorphous halo's position on the temperature can be described by a linear function, the same for all the samples investigated, The temperatures at which the plots become linear during heating are equal to those at which the crystallinity of the samples drops to zero. This fact indicates the close connections between the partially ordered regions in the amorphous phase and the crystallites. Those regions are most probably located in the transition layers between the crystallites and the amorphous phase. The density of those partially ordered regions decreases with the increase in 1-octene content. Such a conclusion results from Figure 4. and from the reciprocal relationship between the amorphous halo position and the average distance between macromolecules in the amorphous phase. We can see that the deflection of plots towards higher angles increases with the decrease in 1-octene concentration and reaches the highest value for pure LPE. The destructive influence of 1-octene co-monomers on the density of partially ordered regions in the amorphous phase is quite obvious: the co-monomers introduced into the structure of the polyethylene macromolecule form short side branches, which disrupt the regularity of the main chain and make closer packing of the chains impossible.

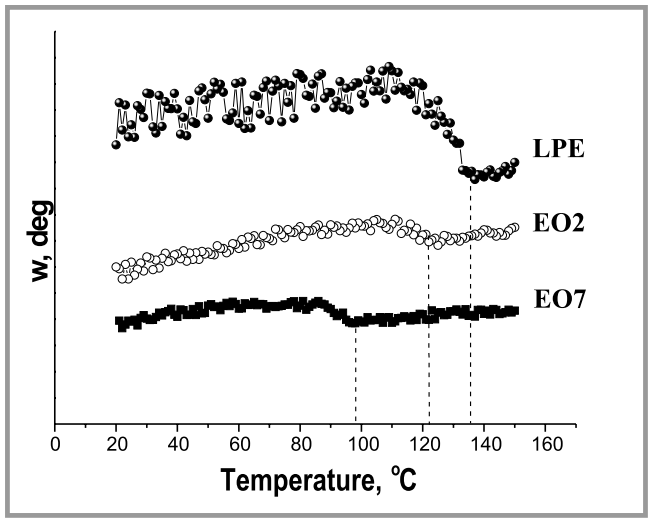


***Figure 7.*** *Width at half height of amorphous halo as a function of temperature during heating. The plots for LPE, EO2 and EO7 are shifted vertically for better visualisation.*

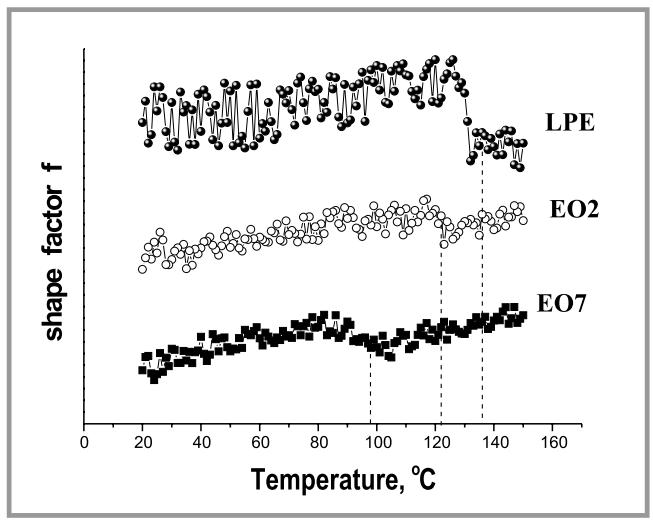


***Figure 8.*** *Shape factor* f *of amorphous halo as a function of temperature during heating. The plots for LPE, EO2 and EO7 are shifted vertically direction for better visualisation.*

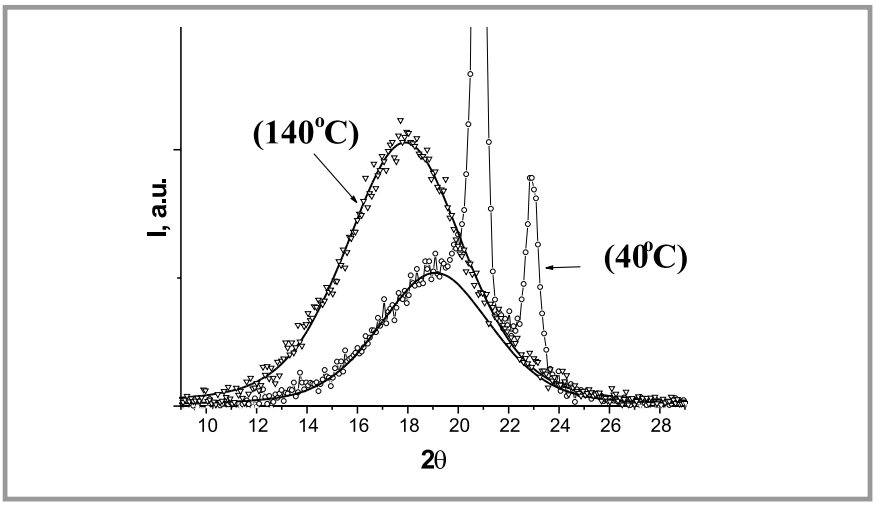


***Figure 9.*** *WAXS patterns for EO2 copolymer at 40°C and 140°C.*

The results presented show that analysis of the shape and angular position of the amorphous halo in WAXS patterns of semicrystalline polymers is a sensitive and fruitful method for obtaining information on the amorphous phase's structure. ❑

## Acknowledgment

*This work was financed by the Polish Committee for Scientific Research - grant № 3 T08E 091 27.*

## References

1. *Swan P. R., J.Polym. Sci 1960,**42**, 525.*
2. *Schröter B., Posern A., Macromol. Chem. Rapid. Commun. **3**, 623, (1982)*
3. *Alexen D.E., Mandelkern l., Popli R., Mathieu P., J. Polym.Sci, Polym Phys.Ed., **21**, 2319, (1983).*
4. *Kitamaru R., Horii F., Murayama K., Macromolecules, **19**, 636, (1986)*
5. *Cheng J., Fone M., Schwartz K.B., Fischer H.P., Wunderlich B., J. Polym.Sci, Polym Phys.Ed.,**32**, 2683,(1994).*
6. *Kitamaru R.,Nakaoki T., Alamo R.G., Mandelkern L., Macromolecules, **29**, 6847, (1996).*
7. *Strobl G., Hagedorn W., J. Polym.Sci, Polym Phys.Ed., **16**, 1181, (1978).*
8. *Glotin M., Mandelkern L., Colloid Polym. Sci. **260**, 182, (1982).*
9. *Shen C., Peacock A.J., Alamo R.G., Vickers T.J., Mandelkern L., Mann C.K., Appl. Spectrosc., **46**, 1226, (1992).*
10. *Wang L.H., Porter R.S., Stidham H.D., Hsu S.L., Macromolecules, **24**, 5535 (1991).*
11. *Mutter R., Stille W., Strobl G., J. Polym.Sci, Polym Phys.Ed., **29**, 99, (1991).*
12. *Voigt-Martin I.G., Alamo R.G., Mandelkern L., J. Polym.Sci, Polym Phys.Ed., **24**, 1283, (1986).*
13. *Suzuki H., Grebowicz J., Wunderlich B., Makromol.Chem.**186**,1109, (1985).*
14. *??[[Von k C.G.]],. J.Appl.Crystallogr. **6**, 81, (1973).*
15. *Ruland W., J.Appl.Crystallogr. **4**, 70, (1971).*
16. *Baker A.M.E., Windle A.H., Polymer, **42**, 667, (2001).*
17. *McFaddin D.C., Russell K.E., Gang Wu, Heydig R.D., J. Polym.Sci, Polym Phys.Ed., **31**, 175, (1993).*
18. *Monar K., Habeschuss A., J. Polym.Sci, Polym Phys.Ed., **37**, 3401, (1999).*
19. *Kelleus M, Meeussen W, Gerkhe R, Reynaers H., Chem.Phys.Lipids; **58**:131, (1991).*
20. *Rabiej M., Polimery **47**, 423 (2002).*
21. *Rabiej M., Polimery **48**, 289, (2003).*
22. *Rabiej M., Rabiej S., this issue.*
23. *Simanke A.G., Alamo R.G., Galland G.B., Mauler R.S., Macromolecules, **34**, 6959, (2001).*
24. *Bartczak Z., Galeski A., Argon A.S., Cohen R.E., Polymer, **37**, 2113, (1996).*
25. *Alexander L.E., X-Ray Diffraction Methods in Polymer Science, Wiley-Interscience, New York 1969 p.381.*

❑ ***Received 08.12.2004 Reviewed 10.02.2005***